APEM journal

Advances in Production Engineering & Management
Volume 21 | Number 1 | March 2026 | pp 75–88
https://doi.org/10.14743/apem2026.1.562

ISSN 1854-6250
Journal home: apem-journal.org
Original scientific paper

A new bilevel model for EV fast charging station location planning with dynamic traffic assignment

Qiu, H.T.[a,*]

[a]School of Management and Engineering, Capital University of Economics and Business, Beijing, P.R. China

A B S T R A C T

Intelligent siting of electric vehicle (EV) fast charging stations is of great significance for the development of urban transportation. This study comprehensively considers factors related to the placement of EV fast charging stations, including differences in travel behavior between fuel vehicle travelers and EV travelers, road congestion, vehicle energy consumption, and the geographical location of charging stations. Based on these factors, an advanced bilevel programming model integrating dynamic traffic assignment (DUE) and charging station location selection is developed. Specifically, the upper level uses a genetic algorithm (GA) to solve a system optimization model aimed at minimizing total travel time while accounting for the construction and operation costs of charging stations. Corresponding to the upper-level decisions, the lower level captures the joint selection behaviors of fuel and electric vehicles and is solved by a DUE procedure combined with the method of successive averages (MSA). This lower-level model incorporates travelers' on-route fast-charging behaviors, including departure time choice, charging facility preference, and route selection. The integrated approach provides a sophisticated framework for analyzing and optimizing the interaction between charging station placement, travel time, and associated costs. An iterative dynamic traffic flow algorithm integrating EV charging queue simulation is proposed. Finally, numerical studies conducted on an illustrative network derive optimal location schemes at different EV adoption stages and analyze the complex operational characteristics of the traffic network under the coexistence of EVs and fuel vehicles.

A R T I C L E   I N F O

Keywords:
Electric vehicles;
Fast charging station;
Bilevel programming;
Location planning;
Siting and sizing;
Dynamic user equilibrium;
Traffic assignment;
Charging queueing;
Logit-based traveler choice

**Corresponding author:*
qiuheting@cueb.edu.cn
(Qiu, H.T.)

Article history:
Received 16 June 2025
Revised 11 March 2026
Accepted 17 March 2026

1. Introduction

Reducing carbon emissions is essential for climate governance, and electric vehicles have emerged as a key solution [1]. Driven by national strategies, the industrialization of electric vehicles in China is advancing rapidly. The development of charging facilities is a crucial part of this process, as it directly influences the adoption rate of electric vehicles. As of June 2024, the ownership of new energy vehicles (NEVs) in China has exceeded 20 million units, with the national cumulative charging infrastructure reaching 9.023 million charging points. Despite the steady growth in the number of charging facilities, surveys indicate that many charging piles suffer from low utilization rates. Due to the uneven distribution of resources, some areas face shortages while others experience oversupply. Currently, the establishment of charging stations across various regions in China remains in the fixed-site demonstration construction phase.

The location planning of charging stations and the charging behavior of EV users profoundly impact traffic flow dynamics [2]. A recent study analyzed TealDrive and Weibo user reviews using sentiment analysis and topic modeling, identifying key themes and stressing the value of user feedback for EV charging infrastructure planning [3]. In daily travel, commuters make decisions not only about route selection but also about departure time, yet existing research inadequately addresses the interplay between charging station placement, traffic network efficiency, and user behavior [4, 5].

Research on charging station (CS) location optimization primarily employs two models: point demand and flow demand [6]. Scholars have expanded these frameworks with optimization methods, such as data-driven geographic grid optimization [7], car sharing [8], spatial-statistical coverage models [9], and spatiotemporal taxi charging layouts [10]. A recent work combined the sparrow search algorithm with backpropagation neural networks to build a driving behavior recognition model, enabling accurate evaluation of the impact of driving behaviors on fuel consumption and offering theoretical support for intelligent transportation system design [11]. Certain researchers adopt long short-term memory-gated recurrent units (LSTM-GRU) to forecast electricity usage, thereby easing pressure on the power grid [12]. Others address demand uncertainty, facility reliability, and charging satisfaction [13], yet most neglect the interaction between CS placement and traffic network efficiency, as well as the impacts of traveler behavior.

Route choice is critical in transportation science, where dynamic traffic assignment (DTA) models analyze network equilibrium. Studies explore path transitions [14], travel behavior [15], urban mobility improvement [16] and mode choice via prospect theory [17]. Recent work integrates EVs into traffic flow analysis, such as coordinated traffic-power network planning [18] and time-varying DTA [19]. Xu *et al*. adopted a mileage-based strategy for CS placement to reduce range anxiety [20], while Riemann *et al*. [21] implemented stochastic user equilibrium in their models. Zheng *et al*. constructed a bi-level model for CS location [22], and Zhang *et al*. predicted the spatiotemporal demand of electric vehicles (EVs) [4]. A multi-criteria decision-making method is also proposed to optimize the route [23]. Sun *et al*. put forward a two-layer partition method that divides heterogeneous congestion networks into sub-regions, establishes a multi-region traffic flow balance model, and uses this model to analyze heterogeneous congestion networks [24]. To solve the electric vehicle routing problem with time windows, Wang *et al*. proposed an integer mixed programming model incorporating time and area prices, which enhanced the model's realism [25]. Huang *et al*. developed a joint optimization model for electric vehicle (EV) battery recharging and scheduling under dynamic electricity prices, aiming to determine optimal charging arrangements (recharging time and quantity) and transportation plans (transportation time and quantity) [26]. In the domain of EV charging behavior modeling, simulation-based approaches have gained increasing attention. Tang *et al*. [27] introduced a Q-learning framework for simulating EV charging station recommendations, dynamically adapting to user behaviors to improve recommendation accuracy and station utilization, highlighting the importance of incorporating user preferences into charging infrastructure planning. For charging station location optimization, Can *et al*. [28] developed a novel approach for electric buses, considering the operational constraints of public transit systems, contributing to the growing literature on differentiated charging infrastructure planning. Despite these efforts, queuing delays, the impedance differences between EVs and fuel vehicles, and the influence of departure times remain unaccounted for in these models.

This study develops a bi-level programming model integrating dynamic user equilibrium (DUE) and system optimal (SO) approaches to optimize fast-charging station locations. The model incorporates EV users' charging behavior (arrival, queuing, and charging) and analyzes mixed traffic networks with both EVs and fuel vehicles. Through a micro-level analysis of departure time choices, route selection, and charging patterns, it examines how travel decisions affect station siting. The research elucidates the interactions among travelers, road network conditions, and charging infrastructure to support optimal station placement decisions.

The remainder of this paper is organized as follows. Section 2 presents the problem description and the formulation of the bilevel programming model for EV fast charging station location planning, including its workflow, assumptions, variable definitions, upper/lower model designs and solution algorithms. Section 3 conducts simulation experiments to validate the model and algorithm, presenting location planning results under different EV penetration rates and analyzing traffic flow assignment and departure time distribution. Section 4 discusses model performance by comparing the DUE and SUE models, and analyzes their differences in charging station planning and road network operation efficiency. Finally, Section 5 summarizes the research conclusions, clarifies the study limitations, and proposes future research directions and practical application suggestions for fast charging station location planning.

2. Problem description and model

2.1 Workflow

The methodology for selecting sites for fast charging stations is depicted in Fig. 1. The bi-level location planning model comprises three key components: travelers' behavior, traffic flow assignment, and the determination of optimal charging station locations and capacities. The study focuses on the impact of traffic on the site selection of charging stations, so dynamic charging demands, the road network, and the characteristics of travelers' behavior are mainly considered. By balancing system-level and individual-level optimization, the model identifies a charging station layout that improves overall network efficiency while also enhancing individual travel utility.

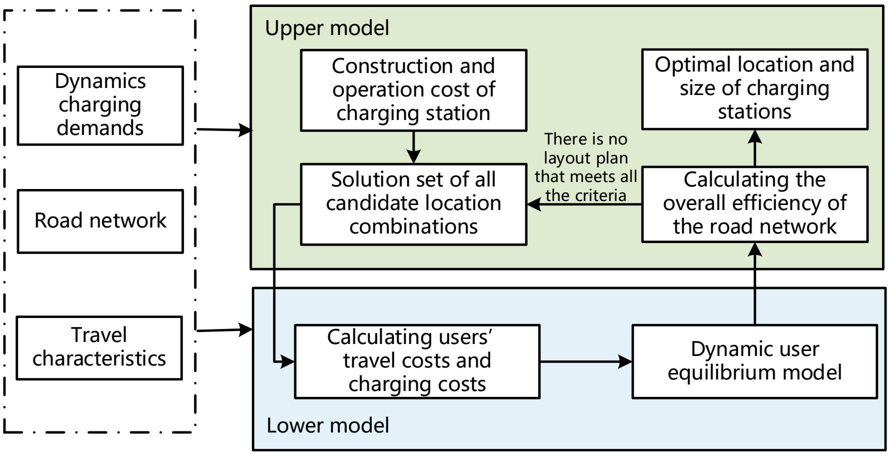

Fig. 1 Process of site selection

2.2 Model assumptions and definitions

This study adopts the following key assumptions: (1) The network includes both EVs and fuel vehicles that select routes based on perceived path resistance. EV drivers optimize charging strategies according to real-time traffic, with energy consumption proportional to the distance traveled. (2) Charging queues form when demand exceeds station capacity. Fast-charging duration follows a normal distribution (this assumption is model-independent). (3) No spatial constraints exist for charger placement, but total construction costs must remain within budget. (4) All network nodes are candidate locations for charging stations. (5) Travelers learn and adapt route choices based on historical travel time data.

To facilitate model development and theoretical validation, this study adopts a deliberate simplification in Assumption (4), treating every network node as a potential charging station site. However, in real-world applications, site feasibility is constrained by multiple factors including land availability and cost, grid connection capacity, zoning regulations, and infrastructure requirements. If only a subset of nodes were feasible, the optimal solution would likely concentrate charging capacity on the remaining feasible nodes, potentially leading to higher congestion at those stations, longer detour distances for EV users, and increased overall network travel time. The model can be extended to incorporate feasibility constraints by adding a binary parameter f_j indicating whether node j is feasible ($f_j = 1$) or not ($f_j = 0$), and modifying the upper-level decision variable such that ω_j can only be 1 if $f_j = 1$. This extension would require additional data collection on node-specific feasibility factors, which we identify as an important direction for future research applying the model to real-world cities.

In this paper, the transportation network is modeled as a graph structure $G = (J, A)$, where J is the set of transportation nodes; A is the set of road segments; a is a road section, $a \in A$; W is the set of origin-destination (OD) pairs in a network, and w is an OD pair in W, $w \in W$; R_w is the set of paths associated with OD pair w, and r denotes one of these paths, $r \in R$. There are two categories of travelers: those who drive electric vehicles, represented by e, and those who drive fuel vehicles, represented by g. The set of vehicle types is denoted as $B = \{b|g, e\}$. The time period $[0, H]$ is discretized to a set of time intervals which contains π time periods, and let ς be the interval length such that $H = \varsigma\pi$. The study period $[0, H]$ is large enough for all peak hour travelers to be able to complete their trips, and the traveler who enters any road section in a certain time period cannot leave the road section in the same time period.

For $\forall t \in [t_1, t_2, \cdots, t_\pi]$, $v_w^{rb}(d,t)$ is the flow of b-type vehicles on the path r at time t of day d v_a^b(d,t) is the flow of b-type vehicles on the link a at time t of day d; $u_a^b(d,t)$ is the inflow of b-type vehicles on the link a at time t of day d; $x_a^b(d,t)$ is the outflow of b-type vehicles on the link a at time t of day d. $T_a(d,t)$ is the travel time of link a at time t on day d, $T_r(d,t)$ is the travel time of route r at time t on day d. $u_{ar}^{wb}(d,t)$, $x_{ar}^{wb}(d,t)$, $v_{ar}^{wb}(d,t)$ are the inflow, outflow and flow of b-type vehicles of link a on route r at time t. In discrete time, the travel time of link a can be expressed as $T_a(\mathrm{d,t}) = [T_a(d,t_1), T_a(d,t_2), \cdots, T_a(d,t_\pi)]$, and the inflow of link a at time $t'(t' \in [t_1, t_1, \cdots, t_\pi])$ can be represented as:

$$u_a(d,t') = \sum_w \sum_r \sum_t \sum_b v_w^{rb}(t) \cdot \varpi_{a,r,t}^{wb}(d,t') \tag{1}$$

The binary variable $\varpi_{a,r,t}^{wb}(d,t')$ denotes the association between link a and route r. Specifically, it takes a value of 1 if travelers departing from the origin at time t can reach link a at time t'; otherwise, $\varpi_{a,r,t}^{wb}(d,t') = 0$.

2.3 Upper model

From the perspectives of charging station construction and traffic management authorities, this section conducts a comprehensive assessment of road network performance, the expenses involved in setting up charging stations, and their impact on existing road conditions. This study establishes a system-optimal objective for the road network and subsequently optimizes the placement and design of charging stations.

Given the notable differences in route choice behaviors between EV and fuel vehicle drivers, the growing adoption of EVs is poised to exert a substantial impact on the operation of the existing traffic network. When the road network is balanced, electric vehicle users will choose the path with the least travel cost. Therefore, decision makers need to consider how to deploy public charging stations to minimize system impedance from a holistic perspective. To balance total travel time minimization with the control of charging station construction and operational costs, the upper-level model employs a dual design combining the objective function and a hard budget constraint: the objective function (Eq. 2) takes the total road network impedance (integrating the travel time of EVs and fuel vehicles) as the core objective to minimize the travel time of the whole network, and the subsequent cost budget constraint (Eq. 3) forms a rigid limit on the total cost, thus realizing a dynamic trade-off between the two optimization objectives. The following model is proposed:

$$min \sum_{r=1}^{R} c_w^r(d,t) = \sum_{r=1}^{R} \left(c_w^{rg}(d,t) + c_w^{re}(d,t) \right) \tag{2}$$

where $c_w^r(d,t)$ denotes the actual path travel impedance for route r between OD pair w on day d at time t, $c_w^{rg}(d,t)$and $c_w^{re}(d,t)$ represent the actual path impedances for fuel vehicles and electric vehicles when they choose path r at time t on day d.

The main constraints include land, construction, and operating costs, as well as the time value of capital. The total annual investment cost is affected by the following factors:

$$\sum_j \omega_j \frac{i(1+i)^Y}{(1+i)^Y - 1} (M_1 + M_2 + M_3) \leq M_{max} \tag{3}$$

Let M_1 denote the land price, M_2 the construction cost, and M_3 the operating cost of the charging station at node j. The discount rate i and service life y are also considered. M_{max} refers to the maximum budget allocated by the government for charging station construction. ω_j is a 0-1 variable; specifically, if there is a charging station at node j, ω_j equals 1; otherwise, it equals 0. The total power capacity of the charging station is positively correlated with the number of charging piles s and the rated power of a single pile, and the construction cost M_2 included in the budget constraint (Eq. 3) is associated with the scale of charging piles configuration, which indirectly forms a hard constraint on the total power capacity of the charging station (the total power capacity cannot be infinitely expanded due to the limit of M_{max}).

2.4 Lower model

From the traveler's perspective, the DUE model incorporates multiple attributes influencing path and departure time decisions for both fuel and electric vehicles. It sets optimal individual objectives for travelers and optimizes charging station layouts. Notably, travelers cannot unilaterally boost the network's overall efficiency by changing travel routes or departure times at any moment; this is called equilibrium.

At time t, travelers choose their routes probabilistically. Based on random utility theory, the Logit model is used to describe route-choice behavior. Accordingly, the probability of path selection can be formulated as follows:

$$P_w^r(d,t) = \frac{\exp(-\theta_1 c_w^r(d,t))}{\sum_{r \in R_w} exp(-\theta_1 c_w^r(d,t))}, w \in W, r \in R_w \tag{4}$$

where $P_w^r(d,t)$ denotes the probability that travelers in OD pair w choose path r at time t on day d, $c_w^r(d,t)$ stands for the path impedance when travelers of OD pair w choose path r at time t on day d, θ_1 is a positive parameter. In view of the different path selection features of fuel vehicles and electric vehicles, separate calculations are performed to determine the path impedances for each vehicle type.

We adopt the Bureau of Public Roads (BPR) function as the selected average link travel time function, and also make use of the real-time traffic flow of the link. The travel impedance of vehicles powered by fuel on path r can be expressed as:

$$c_w^{rg}(d,t) = T_w^g(d,t) + F_r^g \tag{5}$$

where $T_r^g(d,t)$ is the travel time of fuel vehicles on path r at time t on day d, $F_r^g(d,t)$ represents the fuel cost, which can be calculated by the length of the link and the fuel cost per unit distance.

EV travel involves three key components: driving time, charging waiting time, and charging duration. An electric vehicle's overall travel duration is largely determined by driving time, in addition to charging waiting time and actual charging duration. The travel cost of using electric vehicles mainly includes recharging cost and electricity consumption, which can be calculated by multiplying route length by the per-kilometer electricity cost.

The travel duration of EVs on a link is determined by the BPR function. The service process at charging stations follows the M/M/S/K queuing model; specifically, the inter-arrival times of customers follow a negative exponential distribution with parameter λ, there are s service stations, each server's service time is independent and follows a negative exponential distribution with parameter μ, and the system capacity is K. Thus, the M/M/S/K queuing model is used to calculate the waiting time at charging station j.

C_{max} is the maximum charge quantity of electric vehicles, and the residual charge quantity is $C_j(d,t)$ when reaching charging station j at time t on day d. User arrival frequency $\lambda_j(d,t)$ is calculated on the basis of the EV inflow u_a^e(d,t) and the residual battery capacity of EVs on the link a at time t:

$$\lambda_j(d,t) = \begin{cases} 0.8 \cdot u_a^e(d,t)\text{ , if } C_j(d,t) \le C_{max} \cdot 20\ \% \\ 0.6 \cdot u_a^e(d,t)\text{ , if } C_{max} \cdot 20\ \% \le C_j(d,t) \le C_{max} \cdot 40\ \% \\ 0.4 \cdot u_a^e(d,t)\text{ , if } C_{max} \cdot 40\ \% \le C_j(d,t) \le C_{max} \cdot 60\ \% \\ 0.2 \cdot u_a^e(d,t)\text{ , if } C_{max} \cdot 60\ \% \le C_j(d,t) \le C_{max} \cdot 80\ \% \\ 0.1 \cdot u_a^e(d,t)\text{ , if } C_j(d,t) > C_{max} \cdot 80\ \% \end{cases} \tag{6}$$

Let ρ_2 denote the unit charging cost; the total charging fee is $\mathrm{F}_{a1}^e(d,t) = \eta \cdot \rho_2 \cdot T_\Delta(d,t)$, and the electricity consumption cost is $\mathrm{F}_{a2}^e(d,t) = \eta \cdot \rho_2 \cdot s_\mathrm{a}(d,t)$. Of particular relevance is that the arrival rate $\lambda_j(d,t)$ in the queuing model is endogenously determined by the traffic flow from the lower-level DUE model and the residual battery level of EVs, as expressed in Eq. 6. The piecewise coefficients (0.8, 0.6, ⋯) represent a behavioral rule where drivers with lower battery levels are more likely to seek charging, ensuring that queue dynamics are responsive to both traffic conditions and vehicle states.

The service rate μ is derived from the charging time $T_{\Delta}(d,t)$, which is assumed to vary within a reasonable range [0,10] minutes based on typical fast-charging durations. According to the physical relationship $P = E/T$, the charging time implicitly constrains the charging power limit, where E is the charging energy determined by the battery residual capacity and maximum capacity C_{max}.

The number of chargers s is an upper-level decision variable optimized by the genetic algorithm, with its value limited to [3,10]. It directly determines the maximum concurrent service capacity of the charging station and thus forms a hard constraint on the station throughput. Combined with the endogenously determined arrival rate $\lambda_j(d,t)$, the actual station throughput can further match real-time charging demand. For the system capacity K, we assume it is sufficiently large (effectively infinite) in this strategic planning context, as the focus is on long-term location decisions rather than detailed operational queue management. Therefore, the travel impedance of EVs on link A is:

$$c_w^{ae}(d,t) = T_a(d,t) + T_{\Delta}(d,t) + W_{q_j}(d,t) + \mathrm{F}_{a1}^{e}(d,t) + \mathrm{F}_{a}^{e}(d,t) \tag{7}$$

where $W_{qj}(d,t)$ denotes the average waiting time of EVs at charging station j, $T_{\Delta}(\mathrm{d,t})$ is the charging time. The travel impedance of electric vehicles on path r can be formulated as:

$$c_w^{re}(d,t) = \sum_{a\in A}(T_a(d,t) + T_{\Delta}(d,t) + W_{q_j}(d,t) + \mathrm{F}_{a1}^{e}(d,t) + \mathrm{F}_{a}^{e}(d,t)) \tag{8}$$

Travelers choose their departure times randomly. Assuming a continuous distribution, the probability of departure time selection is calculated using the Logit model:

$$\tau_w^r(d,t) = \frac{\exp(\theta_2\varphi_w^r(d,t))}{\sum_{r\in R_w}\exp(\theta_2\varphi_w^r(d,t))}, w \in W, r \in R_w \tag{9}$$

where $\tau_w^r(d,t)$ and $\varphi_w^r(d,t)$ are the probability and utility associated with departing at time t for travelers in OD pair w on day d, θ_2 is a positive parameter reflecting travelers' sensitivity to different departure time choices. It should be noted that the parameters θ_1 and θ_2 in the Logit models are assumed values that satisfy the theoretical condition $\theta_1 > \theta_2$, which guarantees the existence of a unique solution in the discrete choice framework (see [29] for details). The specific values ($\theta_1 = 1$, $\theta_2 = 0.3$) are chosen for model identifiability and are consistent with common practice in transportation behavior studies. As the primary focus of this paper is to demonstrate the theoretical validity and algorithmic feasibility of the proposed bilevel model, the use of assumed parameters is considered acceptable at this stage. Future work should calibrate these parameters using real-world travel survey data.

Based on the value function in prospect theory, the utility function $\varphi_w^r(d,t)$ is defined as follows.

$$\varphi_w^r(d,t) = \begin{cases} \beta_1(t_e - t_a)^{\alpha_1}, & t_a \le t_e \\ \beta_2(t_a - t_e)^{\alpha_2}, & t_e < t_a \le t^* \\ \beta_3(t_s - t_d)^{\alpha_3}, & t^* < t_a < t_s \\ \beta_4(t_a - t_s)^{\alpha_4}, & t_a > t_s \end{cases} \tag{10}$$

Suppose that t_s is the work start time, t is the traveler's acceptable early arrival time, t^* is the traveler's preferred arrival time, and t_a is the traveler's actual arrival time. To calculate the arrival time of a fuel vehicle, the vehicle's departure time and travel time are added. For an electric vehicle, the arrival time is determined by the sum of the departure time, travel time, charging time, and waiting time for an available charging station.

$\beta_1 \sim \beta_4$, $\alpha_1 \sim \alpha_4$ are parameters. Eq. 10 indicates that if a traveler arrives before t, there is an early arrival penalty; if the traveler arrives after t_s, there is a late arrival penalty. If a traveler arrives within $[t, t_s]$, the traveler gains utility. t^* is the preferred arrival time, at which the traveler obtains the greatest benefit. According to the initial theory of Kahneman and Tversky [30], the parameter values are as follows: $\beta_1 = -1$, $\beta_2 = \beta_3 = 2.25$, $\beta_4 = -1$, $\alpha_1 = \alpha_3 = \alpha_4 = 0.88$, $\alpha_2 = 0.57$. Combined with Eqs. 4 and 9, the joint choice of departure time and travel path can be expressed as:

$$v_w^r(d,t) = D_w \cdot P_w^r(d,t) \cdot \tau_w^r(d,t), w \in W, r \in R_w \tag{11}$$

where $v_w^r(d,t)$ represents the number of vehicles on path r at t time of day d, and D_w is the total demand of the road network. $v_w^r(d) = D_w \cdot P_w^r(d,t)$ represents the total flow of the two types of vehicles on path r for each departure time of the day. $v_w(d,t) = D_w \cdot \tau_w^r(d,t)$ is the total flow of the two vehicle types for each departure time of the day.

Departure time and route selection are sequentially interdependent: the selected departure time affects the dynamic route-choice process, and the resulting route selection in turn affects subsequent departure-time decisions. Travelers need to take the interactive effects of these two factors into account when making optimal travel decisions.

2.5 Solution algorithms

The heuristic algorithm is designed based on the method of successive averages (MSA) and a genetic algorithm. The key to the algorithm is the use of the Logit model to derive the route choice probabilities and departure time selection probabilities of the traveler group, followed by iterations using the MSA algorithm.

Firstly, the initial population (charging station distribution) is formed by selecting the decision variables of the upper-level model based on a genetic algorithm, and the Logit stochastic dynamic user equilibrium (DUE) model of the lower level is solved based on the charging station distribution. For each charging station distribution in the population, the MSA algorithm is used to calculate the traffic flow assignment at different departure times. Once the equilibrium state is achieved, the path flow is updated and fed into the upper-level model, with well-adapted individuals screened out by means of the fitness function. These selected individuals are then imported into the lower-level programming, and the cycle is repeated to seek the global optimal solution. The steps are as follows:

Step1: Initialization. All simple acyclic paths between OD pairs w are considered as the set of valid paths R_w.

Step2: Outer-loop iteration (Genetic Algorithm). The location and capacity of charging stations are digitally coded to form the initial population, where X represents the number of iterations.

Step3: Inner-loop iteration (Path selection and departure time selection). x is the number of iterations.

Step 3.1: Initial path flows for each departure time on the first day are acquired by initializing the path selection probabilities of fuel vehicles and EVs. Path impedances for the two vehicle types are calculated separately for each departure time on the first day.

Step 3.2: Path travel times are computed separately for fuel vehicles and electric vehicles respectively. Subsequently, travelers' utility values for different departure times are calculated according to Eq. 10.

Step 3.3: Path inflow calculations. The path inflow is computed using Eqs. 4 and 9. Subsequently, both the path flow and departure time flow are iteratively updated through the MSA algorithm.

Step 3.4: Convergence check. The iteration terminates when the traffic flow assignment reaches an equilibrium state, satisfying the convergence criteria: $v_w^{r(x)}(d) - v_w^{r(x-1)}(d) \leq \delta$ and $v_w^{r(x)}(d,t) - v_w^{r(x-1)}(d,t) \leq \delta$, where δ represents the predetermined error threshold. If converged, proceed to Step 4; otherwise, return to Step 2 for further iterations.

Step 4: Construct the fitness function and start the genetic algorithm. Digital coding is used to represent the location and capacity of charging stations, with each chromosome corresponding to a specific layout of charging stations. In the crossover and mutation phases, the roulette wheel selection method is applied to pick chromosomes for generating a new population. The set crossover probability is 0.8 and the mutation probability is set at 0.01. For instance, the quantity of charging piles is limited to the range of [3,10].

Step 5: Termination criterion for the genetic algorithm: The iterative optimization process terminates when the condition $\max F^{(X+1)} - \max F^{(X)} < \varepsilon$ is satisfied for generation X, where ε represents the predefined convergence threshold. If not, the algorithm reverts to Step 2 to proceed with the evolutionary iteration process.

3. Simulation experiments and results

3.1 Simulation setup

A test network is adopted in this study to verify the validity of the proposed model and algorithm, whose structure is presented in Fig. 2 and comprises 9 nodes, 12 links and 6 paths. Network nodes are set as optional locations for charging stations, and the number of charging piles configured for each station is in the range of 3 to 10. The initial battery capacity of electric vehicles conforms to a normal distribution of $\mathcal{N}(120,\ 3.6^2)$.

There are six paths in the road network, as shown in Table 1. The initial simulation parameters are presented in Tables 2, 3 and 4.

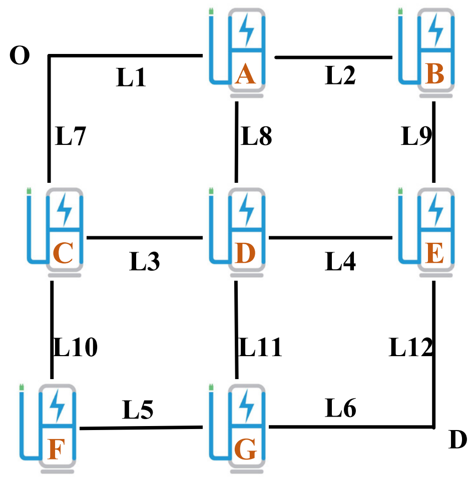

Fig. 2 The example network

Table 1 Paths

Path design	
Path 1: L1 - L2 - L9 - L12	Path 2: L1 - L8 - L4 - L12
Path 3: L1 - L8 - L11 - L6	Path 4: L7 - L3 - L4 - L12
Path 5: L7 - L3 - L11 - L6	Path 6: L7 - L10 - L5 - L6

Table 2 Network parameters

Link	L_a	T_a^0	Link	L_a	T_a^0
1	50	10	7	50	10
2	32	10	8	64	12
3	50	12	9	32	10
4	64	10	10	32	12
5	50	14	11	64	8
6	64	10	12	32	10

Table 3 Model parameters

Parameters	Value	Parameters	Value	Parameters	Value
θ_1	1	θ_2	0.3	ς	10 min
ρ_1	0.6	ρ_2	0.016	D_w	200
C_{max}	200	δ, ε	0.01	i	8 %
$T_\Delta(d,t)$	[0,10]	π	6	η	1.47
t_e	9:00	t^*	9:25	t_s	9:35
Y	20	γ	0.1	M_{max}	20 million

Table 4 Areas of supporting facilities

Functional zone	Area (m^2)	Functional zone	Area (m^2)	Functional zone	Area (m^2)
Transformer room	50	High voltage distribution room	50	Control room	40
Low voltage distribution room	100	Charging set room	60	Service zone	50

3.2 Location planning results

Based on the experimental road network, the optimal scheme for charging station siting and capacity configuration under various electric vehicle penetration rates is derived, as presented in Table 5. The charging station layout aims to maximize the travel utility of users and minimize the overall travel time of the network. The total travel demand of the road network is 200. A–G denotes the charging station index, and the values in the corresponding columns represent the number of charging piles at each station.

According to Table 5, when the EV penetration rate reaches 20 %, the number of charging stations begins to increase to ensure road network efficiency. Yet, with further increases in the number of electric vehicles, efficient charging can be maintained through traffic flow optimization, eliminating the need for additional piles.

Once the local EV penetration rate exceeds 50 %, new charging stations become crucial for network efficiency. The maximum number of charging stations is reached when the electric vehicle density hits 70 %. To optimize charging station placement under rising EV adoption and declining numbers of conventional vehicles, an approach that accounts for departure times and route choices is recommended. This strategy meets charging demands, boosts traffic efficiency, and reduces the number of required stations. Notably, no fixed correlation exists between the number of charging stations and the number of electric vehicles. Optimizing station layout and traffic flow can enhance road network efficiency with fewer stations, rather than simply adding more infrastructure.

Notably, the optimization results of charging station locations in Table 5 also reflect the adaptive adjustment characteristics of the model to the cost-travel time weight: the change of the total number of charging piles with the EV penetration rate is essentially the model's dynamic trade-off between meeting the traffic efficiency demand (reducing travel time) and controlling the construction and operation costs under the fixed budget constraint M_{max}.

Table 5 Location planning results of CS with different penetration rate of EVs

Penetration rate of EVs (%)	A	B	C	D	E	F	G	Total number of charging piles
10	6	5	9	0	5	0	0	25
20	5	5	6	10	8	0	0	34
30	7	5	3	0	10	0	0	25
40	4	3	5	5	7	0	0	24
50	7	7	6	0	5	0	0	25
60	0	8	10	9	5	0	0	32
70	8	9	10	8	6	0	0	41
80	6	9	10	6	4	0	0	35
90	3	0	0	4	0	6	8	21

3.3 Analysis of traffic flow assignment

Tables 6 and 7 illustrate the travel times and selection probabilities of routes for these vehicles at EV proportions of 10 %, 50 %, and 90 %. As shown in Table 6, Paths 1, 3, and 5 have the shortest travel times and the highest route selection probabilities for fuel vehicles. Path 6 has the longest travel time and the lowest selection probability, aligning with the expected utility theory. Notably, at a 50 % EV proportion, Paths 3 and 5 have equal travel times. With 7 charging piles on Path 3 and 6 on Path 5, Path 5 has a higher traffic flow ratio, indicating that fuel vehicles prefer paths with fewer charging piles when travel times are the same.

Table 6 Travel time and path selection of each path for fuel vehicles

Path	Penetration rate of EV								
	10 %			50 %			90 %		
	Travel time	Routing (%)	Number of CPs	Travel time	Routing (%)	Number of CPs	Travel time	Routing (%)	Number of CPs
1	40.6	18.9	16	40.2	19.3	19	40.4	20.4	3
2	42.0	13.9	11	42.2	13.8	12	42.3	14.6	7
3	40.0	21.6	6	40.1	22.1	7	40.3	21.5	15
4	42.0	14.1	14	42.3	14.0	11	42.6	14.4	4
5	40.1	22.1	9	40.1	22.5	6	40.2	21.2	12
6	46.5	9.4	9	46.3	8.3	6	46.6	7.9	14

From Table 7, at a 90 % EV proportion, Path 1 has the shortest travel time, the fewest charging piles, and the lowest traffic flow share. Despite being second in travel time among the six routes, Path 3 has the highest flow distribution ratio due to its largest number of charging piles, suggesting that EV travelers prioritize charging station layout and convenience when choosing routes.

When the EV proportion is 50 %, Path 1 has the highest traffic flow allocation. Its travel time ranks second among the six paths, yet it has the most charging piles. Evidently, at this EV penetration rate, charging stations influence route selection more than travel time.

At a 10 % EV proportion, Path 6 has the longest travel time and the lowest traffic flow share, in line with the expected utility theory. Path 1 has the shortest travel time, but Path 5 has the largest traffic flow allocation proportion, conforming to the principle of random user equilibrium. When Path 1 has far more charging piles than Path 5, the probability of choosing Path 5 is higher, showing that at a 10 % EV proportion, the number of charging piles affects path selection less than travel time.

According to the above results, the location of charging stations has a significant impact on user behavior and the distribution of traffic flow in the road network, which in turn affects the traffic efficiency of the road network.

Table 7 Travel time and path selection of each path for electric vehicles

Path	Penetration rate of EV								
	10 %			50 %			90 %		
	Travel time	Routing (%)	Number of CPs	Travel time	Routing (%)	Number of CPs	Travel time	Routing (%)	Number of CPs
1	59.3	18.6	16	60.1	18.9	19	60.1	7.6	3
2	61.9	18.3	11	62.1	18.3	12	62.0	18.7	7
3	60.0	18.7	6	60.3	18.8	7	60.2	19.2	15
4	62.0	18.2	14	61.8	18.2	11	62.2	17.9	4
5	60.1	18.8	9	60.0	18.7	6	60.4	18.3	12
6	66.6	7.3	9	65.9	7.1	6	66.1	18.2	14

Note: The travel time of an electric vehicle is the sum of the driving time, charging time and charging waiting time of the path

3.4 Analysis of departure time distribution

Table 8 shows the traffic distribution of all travelers at different departure times. Fig. 3 shows the departure time selection results of fuel vehicle travelers and electric-vehicle travelers during the morning rush hour. Obviously, there are significant differences in departure times for different types of vehicle users.

From Fig. 3, it can be observed that fuel vehicles predominantly depart at 8:30 and 8:40, whereas electric vehicles are concentrated at 8:10 and 8:20. This paper assumes that the working time is 9:35 and the optimal arrival time is 9:25. Given that the average travel time of fuel vehicles is 42 minutes and electric vehicles have an average travel time of 62 minutes, the departure time for electric vehicles generally needs to be earlier than that for fuel vehicles to arrive before the start of work. The sensitivity of travelers to departure time proves the validity of the utility function designed in this paper. Combined with the distribution of travelers' departure time selections and the analysis of the utility function of travelers' departure time selection, it can be seen that, in order to make the arrival time close to the optimal arrival time of 9:25, travelers adjust their departure times, which conforms to expected utility theory.

Table 8 Flow distribution at different departure times

Departure time	Penetration rate of EV (%)								
	10	20	30	40	50	60	70	80	90
8:00	1	1	1	1	2	3	4	4	40
8:10	3	4	5	24	10	18	38	40	28
8:20	10	17	24	14	37	35	24	28	19
8:30	24	20	15	11	13	15	12	12	6
8:40	51	50	49	46	34	26	20	13	7
8:50	10	8	6	4	4	4	3	3	1

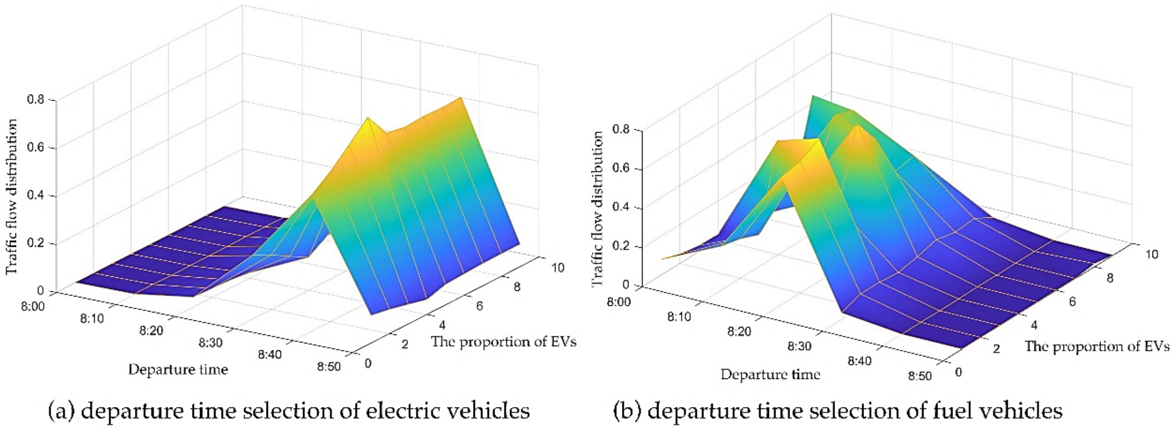

Fig. 3 Choice of departure times of fuel vehicles and electric vehicles

4. Discussion

In previous research, the stochastic user equilibrium (SUE) model is used to characterize travelers' path selection behavior without considering the time-varying nature of the dynamic road network or departure time selection. To compare the effects of the SUE and DUE models, a comparative analysis is conducted. By comparing the number of charging piles (Fig. 4), the vacancy rate, and network travel time under the DUE and SUE models, it can be seen that the DUE model describes traveler behavior more realistically and yields a more plausible charging station planning result.

Upon comparing the results of the DUE and SUE models, it was found that there was no significant difference in the total number of charging stations between the two models. However, as the electric vehicle penetration rate increased, the trend in the number of charging stations varied significantly between the two models. While the SUE model showed a decline in the number of charging stations with the rise in the EV penetration rate, the DUE model exhibited a gradual increase until the 60 % threshold, reaching its peak at 70 % adoption before decreasing. The results show that the DUE model, after considering the effects of departure time selection and dynamic traffic flow assignment on route selection and charging station queuing, yields a more practically relevant charging station planning scheme.

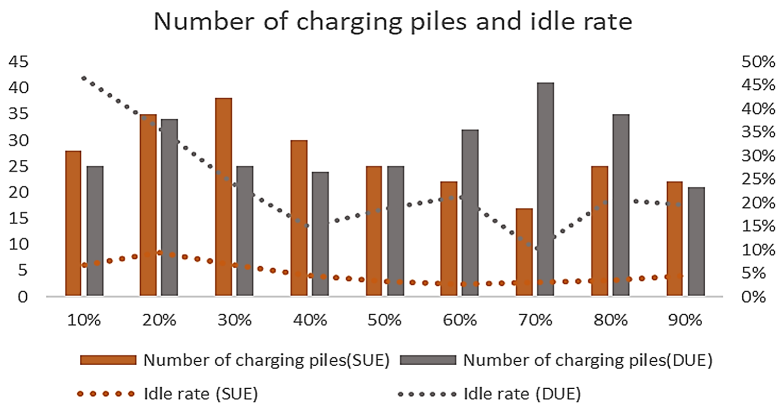

Fig. 4 Optimization results of charging pile number and idle rate

Moreover, a comparison of Fig. 5 shows that the total road network travel time derived from the DUE model is much lower than that derived from the SUE model under any EV penetration rate. However, the vacancy rate of the SUE model is much lower than that of the DUE model. This indicates that in the DUE model, electric vehicle users and fuel vehicle users depart in different time periods because travelers can choose their departure times and different types of travelers have different travel utilities. Under cost constraints, the DUE model significantly reduces the travel time of the road network at the expense of more charging piles and vacancy rates of 10-20 %.

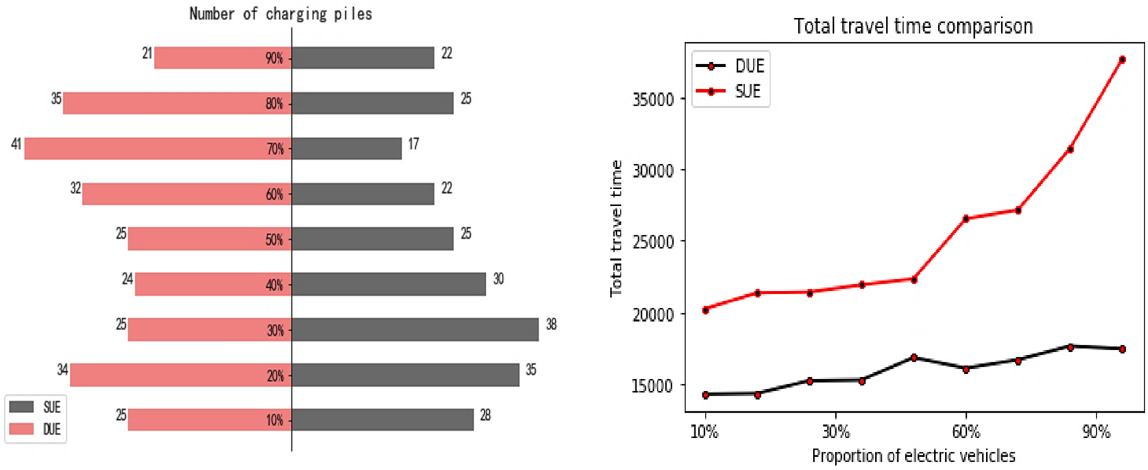

Fig. 5 Comparative analysis of DUE and SUE model results

5. Conclusion

This paper constructs impedance functions for electric and fuel vehicles by considering travel time, energy consumption, charging service, and waiting time. It combines dynamic traffic flow distribution with charging station site selection to create a two-level programming model. By balancing overall and individual optimization, the charging station layout can achieve high traffic efficiency for the overall road network while maximizing individual travel utility. Dynamic user equilibrium theory is used in charging station layout planning to establish a traffic flow allocation model and a solution algorithm for simultaneous departure time and travel path selection, and numerical simulations demonstrate the validity and practicability of the model and algorithm.

The results show the following: (1) High traffic network efficiency does not require adding more charging piles. Optimizing the charging station layout can achieve greater road network efficiency with fewer piles, and the layout significantly impacts road network traffic flow distribution and efficiency. (2) The simulation results are consistent with expected utility theory and stochastic user equilibrium. When the proportion of electric vehicles is low, travel time affects route selection more; when it is high, the number of charging stations matters more. (3) During the morning rush hour, fuel vehicles mainly depart at 8:30-8:40, while electric vehicles do so at 8:10-8:20, validating the effectiveness of the designed departure-time selection utility function.

Constrained by computational complexity and data availability, this study conducts numerical experiments on a 9-node illustrative network to validate the theoretical soundness and algorithmic feasibility of the proposed model. Notably, the scalability of the approach to large-scale networks with hundreds or thousands of nodes requires further investigation. As network size expands, computational complexity increases drastically, primarily stemming from three core factors: the exponential growth of path enumeration, the scaling of the lower-level MSA-based DUE traffic assignment process with the number of nodes, links, and time intervals, and the nested genetic algorithm structure in the upper level—whose time complexity rises significantly with population size and the number of iterations.

Given these challenges, the current implementation is most suitable for strategic planning in medium-sized networks (e.g., up to 50-100 nodes). However, these limitations are not insurmountable. By integrating well-established large-scale optimization techniques—such as path-set reduction methods (e.g., column generation or k-shortest path algorithms), parallel computing, network aggregation strategies, and more efficient metaheuristics (e.g., particle swarm optimization)—the model can be enhanced to maintain acceptable solution quality and computational efficiency when handling large-scale networks. Regarding solution quality, while genetic algorithms are adept at finding near-optimal solutions, global optimality cannot be guaranteed; in large-scale networks, solution quality will be highly dependent on parameter tuning and convergence criteria.

Therefore, future research should test the model on real-world networks (e.g., city-scale networks) using high-performance computing and compare its results with those of other metaheuristics or commercial solvers to systematically evaluate its scalability and solution quality. Such research based on real data will hold significant practical value, with the potential to optimize network traffic efficiency and driving experiences. At the practical application level, administrative authorities can dynamically adjust the service availability and operational strategies of charging stations based on the proportion of electric vehicles on different routes.

Another important consideration for practical application is demand uncertainty. In this study, both the total OD demand D_w and the EV penetration rate are treated as deterministic inputs. However, in reality, these factors may fluctuate from day to day due to various reasons such as special events, weather conditions, or seasonal variations. Under demand uncertainty, the optimal station locations derived from a deterministic model may not perform consistently across all scenarios. High-demand days could lead to severe congestion at certain stations, while low-demand days might result in underutilized infrastructure.

Future research should extend the current framework to account for demand uncertainty. Possible approaches include (1) scenario-based stochastic programming, where multiple demand scenarios are defined with associated probabilities and the objective is to minimize expected total travel time; (2) robust optimization, which seeks locations that perform well under worst-case demand realizations; and (3) sensitivity analysis to evaluate the robustness of deterministic solutions under demand perturbations. Incorporating these methods would enhance the model's applicability to real-world planning, where demand variability is inevitable.

For practical planning of fast charging stations, planners can determine the weight allocation of travel time and construction/operation costs according to the regional traffic development goals and fiscal budget capacity. For traffic-congested urban core areas, the weight of travel time minimization should be appropriately increased (with a moderate relaxation of the cost budget) to deploy charging piles at key traffic nodes and disperse charging demand; for suburban areas or regions with tight fiscal budgets, the weight of cost control should be prioritized to optimize the layout of charging stations at high-demand nodes to achieve cost-effective resource allocation. In specific operation, the weight can be quantified by calibrating the unit travel time delay cost coefficient based on regional traffic survey data and local fiscal expenditure standards for charging infrastructure, to make the weight setting more in line with the actual development needs.

References

[1] Liu, T. (2024). Time-varying influence of policy risk on carbon emissions analysis, *Journal of Service, Innovation and Sustainable Development*, Vol. 5, No. 2, 95-115, doi: 10.33168/SISD.2024.0206.

[2] Türkeş, M., Acatrinei, C. (2024). The effect of drivers and barriers on electric vehicle usage in Romania: Findings from PLS-SEM and MGA, *Economic Computation and Economic Cybernetics Studies and Research*, Vol. 58, No. 4, 195-209, doi: 10.24818/18423264/58.4.24.12.

[3] Yang, X., Xiang, K., Yuan, S., Huang, J. (2024). Vehicle driving behavior recognition and optimization strategies based on cloud computing and SSA-BP algorithm, *Studies in Informatics and Control*, Vol. 33, No. 3, 17-28, doi: 10.24846/v33i3y202402.

[4] Qian, Z., Yi, Z., Zhong, W., Yue, H., Yaojia, S. (2021). Siting and sizing of electric vehicle fast-charging station based on quasi-dynamic traffic flow, *IET Renewable Power Generation*, Vol. 15, No. 18, 4204-4214, doi: 10.1049/iet-rpg.2020.0439.

[5] Vijūnė, J. (2023). Identification of strategic directions for change management in social services sector, *Journal of Service, Innovation and Sustainable Development*, Vol. 4, No. 2, 91-105, doi: 10.33168/SISD.2023.0208.

[6] Li, S., Huang, Y., Mason, S.J. (2016). A multi-period optimization model for the deployment of public electric vehicle charging stations on network, *Transportation Research Part C: Emerging Technologies*, Vol. 65, 128-143, doi: 10.1016/j.trc.2016.01.008.

[7] Vazifeh, M.M., Zhang, H., Santi, P., Ratti, C. (2019). Optimizing the deployment of electric vehicle charging stations using pervasive mobility data, *Transportation Research Part A: Policy and Practice*, Vol. 121, 75-91, doi: 10.1016/j.tra.2019.01.002.

[8] Sarnvanichpitak, T., Mangmeechai, A. (2024). Regional differences in car sharing adoption: Integrating TAM and TPB in Bangkok and Eastern Economic Corridor, Thailand, *Journal of Logistics, Informatics and Service Science*, Vol. 11, No. 12, 71-89, doi: 10.33168/JLISS.2024.1204.
[9] Dong, G., Ma, J., Wei, R., Haycox, J. (2019). Electric vehicle charging point placement optimisation by exploiting spatial statistics and maximal coverage location models, *Transportation Research Part D: Transport and Environment*, Vol. 67, 77-88, doi: 10.1016/j.trd.2018.11.005.
[10] Bhanu, M., Priya, S., Moreira, J.M., Chandra, J. (2023). ST-AGP: Spatio-temporal aggregator predictor model for multi-step taxi-demand prediction in cities, *Applied Intelligence*, Vol. 53, No. 2, 2110-2132, doi: 10.1007/s10489-022-03475-7.
[11] Tang, M., Cao, J., Fan, Z., Gong, D., Xue, G. (2024). Public perceptions of EV charging infrastructure: A combined sentiment analysis and topic modeling approach, *Studies in Informatics and Control*, Vol. 33, No. 2, 59-72, doi: 10.24846/v33i2y202406.
[12] Xia, T., Zhan, S., Xu, J., Ren, X. (2024). An electric vehicle charging control system using LSTM encoding-GRU decoding, *Tehnički Vjesnik – Technical Gazette*, Vol. 31, No. 5, 1530-1535, doi: 10.17559/TV-20230708000789.
[13] Huang, Y., Li, T., Wang, X., Wu, B. (2024). A consumer expectation-based multiple satisfaction model for battery swapping station deployment, *Economic Computation and Economic Cybernetics Studies and Research*, Vol. 58, No. 3, 193-209, doi: 10.24818/18423264/58.3.24.12.
[14] Mounce, R., Carey, M. (2011). Route swapping in dynamic traffic networks, *Transportation Research Part B: Methodological*, Vol. 45, No. 1, 102-111, doi: 10.1016/j.trb.2010.05.005.
[15] Zhu, Z., Zhu, S., Sun, L., Mardan, A. (2024). Modelling changes in travel behaviour mechanisms through a high-order hidden Markov model, *Transportmetrica A: Transport Science*, Vol. 20, No. 1, 1-27, doi: 10.1080/23249935.2022.2130731.
[16] Suryani, E., Hendrawan, R.A., Adipraja, P.F.E., Indraswari, R. (2020). System dynamics simulation model for urban transportation planning: A case study, *International Journal of Simulation Modelling*, Vol. 19, No. 1, 5-16, doi: 10.2507/IJSIMM19-1-493.
[17] Tian, L., Yang, Q., Huang, H., Lü, C. (2016). The cumulative prospect theory-based travel mode choice model and its empirical verification, *Systems Engineering – Theory & Practice*, Vol. 36, No. 7, 1778-1785, doi: 10.12011/1000-6788(2016)07-1778-08.
[18] Wang, X., Shahidehpour, M., Jiang, C., Li, Z. (2019). Coordinated planning strategy for electric vehicle charging stations and coupled traffic-electric networks, *IEEE Transactions on Power Systems*, Vol. 34, No. 1, 268-279, doi: 10.1109/TPWRS.2018.2867176.
[19] Zhou, Z., Zhang, X., Guo, Q., Sun, H. (2021). Analyzing power and dynamic traffic flows in coupled power and transportation networks, *Renewable and Sustainable Energy Reviews*, Vol. 135, Article No. 110083, doi: 10.1016/j.rser.2020.110083.
[20] Xu, M., Yang, H., Wang, S. (2020). Mitigate the range anxiety: Siting battery charging stations for electric vehicle drivers, *Transportation Research Part C: Emerging Technologies*, Vol. 114, 164-188, doi: 10.1016/j.trc.2020.02.001.
[21] Riemann, R., Wang, D.Z.W., Busch, F. (2015). Optimal location of wireless charging facilities for electric vehicles: Flow-capturing location model with stochastic user equilibrium, *Transportation Research Part C: Emerging Technologies*, Vol. 58, Part A, 1-12, doi: 10.1016/j.trc.2015.06.022.
[22] Zheng, H., He, X., Li, Y., Peeta, S. (2017). Traffic equilibrium and charging facility locations for electric vehicles, *Networks and Spatial Economics*, Vol. 17, No. 2, 435-457, doi: 10.1007/s11067-016-9332-z.
[23] Kurnia, A., Oktavia, T. (2024). A multi-criteria decision approach for optimized route planning in retail distribution, *Journal of Logistics, Informatics and Service Science*, Vol. 11, No. 9, 37-53, doi: 10.33168/JLISS.2024.0903.
[24] Sun, H., Zhang, X., Li, D., Tan, J. (2024). Research on intelligent traffic congestion degree collaborative algorithm and path planning based on sensor data, *Tehnički Vjesnik – Technical Gazette*, Vol. 31, No. 4, 1154-1162, doi: 10.17559/TV-20240227001353.
[25] Wang, D.L., Ding, A., Chen, G.L., Zhang, L. (2023). A combined genetic algorithm and A* search algorithm for the electric vehicle routing problem with time windows, *Advances in Production Engineering & Management*, Vol. 18, No. 4, 403-416, doi: 10.14743/apem2023.4.481.
[26] Huang, A.Q., Zhang, Y.Q., He, Z.F., Hua, G.W., Shi, X.L. (2021). Recharging and transportation scheduling for electric vehicle battery under the swapping mode, *Advances in Production Engineering & Management*, Vol. 16, No. 3, 359-371, doi: 10.14743/apem2021.3.406.
[27] Tang, M.C., Cao, J., Gong, D.Q., Xue, G., Khoa, B.T. (2024). Simulation modelling of electric vehicle charging recommendations based on Q-learning, *International Journal of Simulation Modelling*, Vol. 23, No. 3, 495-506, doi: 10.2507/IJSIMM23-3-CO11.
[28] Can, C., Kilic, F., Kaya, Y. (2025). A novel approach for location planning of fast-charging stations for e-buses, *International Journal of Simulation Modelling*, Vol. 24, No. 2, 213-224, doi: 10.2507/IJSIMM24-2-714.
[29] Ben-Akiva, M.E., Lerman, S.R. (1985). *Discrete choice analysis: Theory and application to travel demand*, MIT Press, Cambridge, Massachusetts, USA.
[30] Kahneman, D., Tversky, A. (1979). Prospect theory: An analysis of decision under risk, *Econometrica*, Vol. 47, No. 2, 263-291, doi: 10.2307/1914185.